IECE Transactions on Power Electronics and Industrial Systems
http://dx.doi.org/10.62762/TPEIS.2024.125048

RESEARCH ARTICLE

A Novel Time-Variant State of Charge Estimation Based on an Extended Kalman Filtering Algorithm and Dynamic High-Order Modeling of Lithium-Ion Batteries

Islam Md Monirul[1], Li Qiu[1,*], Inam Ullah[2], Khongorzul Dashdondov[3], Rehan Ali Khan[4] and Amin Sharafian[1]

[1] College of Mechatronics and Control Engineering, Shenzhen University, Shenzhen 518060, China
[2] Department of Computer Engineering, Gachon University, Seongnam 13120, Republic of Korea
[3] Department of Computer Engineering, College of Electrical & Computer Engineering, Chungbuk National University, Republic of Korea
[4] Department of Electrical Engineering, University of Science & Technology, Bannu 28100, Pakistan

Abstract

Accurately determining the state of charge (SOC) is a critical factor in effective energy management for electric vehicles (EVs). Therefore, SOC variations in battery packs must be assessed with high precision. To simulate the complex processes within EVs that involve lithium-ion batteries (LIBs), an appropriate battery model is essential. Accurate parameter extraction through algorithmic methods is key to reliable SOC estimation. A dynamic, high-order equivalent circuit model, featuring two RC pairs in series with the battery's internal resistance, is employed to enhance parameter extraction. The values of the RC pairs are derived by solving equations that characterize the operational states of the high-order circuit. Parameter identification is facilitated by the hybrid pulse power characterization test, which enables precise SOC estimation. The estimation process is further refined by integrating an extended Kalman filter (EKF) technique, along with open-circuit voltage computations. Simulation results demonstrate that this optimization strategy significantly improves SOC estimation accuracy, reducing the initial error to below 2.64% using the EKF approach, compared to a maximum battery model error of 3.88%. As a result, high performance is obtained from LIB packs.

Keywords: extended kalman filter, high-order equivalent model, Lithium-ion batteries, state of charge, parameter identification.

1 Introduction

The persistent dependence on fossil fuels and the increasing effects of environmental challenges have led to a global energy crisis and pressing pollution issues [1]. In response, governments globally are significantly investing in advancing renewable energy

Academic Editor:
Keshav Kaushik

Submitted: 03 November 2024
Accepted: 21 February 2025
Published: 09 March 2025

Vol. 1, **No.** 1, 2025.
10.62762/TPEIS.2024.125048

***Corresponding author:**
✉ Li Qiu
qiuli@szu.edu.cn

Citation
Monirul, I.M., Qiu, L., Ullah, I., Dashdondov, K., Khan, R.A., & Sharafian, A. (2025). A Novel Time-Variant State of Charge Estimation Based on an Extended Kalman Filtering Algorithm and Dynamic High-Order Modeling of Lithium-Ion Batteries. *IECE Transactions on Power Electronics and Industrial Systems*, 1(1), 1–14.

to update conventional energy infrastructures. The automotive industry, a principal source of pollution, is seeing a substantial transition, with electric vehicles (EVs) gaining preference over traditional fuel-powered vehicles [2]. Lithium-ion batteries (LIBs) recognized for their compact size, low maintenance cost, extended life cycles, and elevated energy density, have emerged as the preferred energy source for EVs and energy storage applications [3–5]. Precise assessment of the state of charge (SOC) is essential for optimal battery management, facilitating efficient energy use and averting harm from overcharging or over-discharging [6, 7]. As SOC cannot be directly quantified in LIBs, it must be deduced from external characteristics, rendering accurate SOC estimation a pivotal research priority.

Multiple techniques for SOC estimate have been established and classified into four primary categories: coulomb counting (CC) [8], open circuit voltage (OCV) [9], data-driven methodologies [10, 11], and model-based approaches [12]. The CC method determines SOC by integrating current over time, providing efficiency and expedience [13]. Nevertheless, it is acutely sensitive to the beginning SOC values and the precision of current sensors, potentially resulting in cumulative inaccuracies [14]. Conversely, the OCV technique employs comprehensive experimental data to formulate a correlation between OCV and SOC, yielding more reliable estimates. However, its precision is constrained by hysteresis effects, and it necessitates extended rest periods for open-circuit voltage stabilization, making it inappropriate for real-time applications [15, 16].

Data-driven methodologies assess SOC utilizing comprehensive metrics including temperature, voltage, and current, circumventing the intricacies of battery chemistry and architecture. These methodologies employ sophisticated models such as fuzzy logic [17, 18], support vector machines [19], and neural networks [20–23], to get elevated accuracy and efficiency. Nonetheless, they frequently necessitate high-quality data, intricate designs, and considerable calculation resources [24–26].

Model-based approaches, including sophisticated filtering algorithms, provide substantial benefits for SOC estimates. In contrast to conventional methods such as OCV and CC, model-based approaches provide real-time SOC estimation with less measurement data and reduced processing expenses [1]. As a result, they are extensively utilized in LIB applications, particularly via electrochemical models (EMs) [2] and equivalent circuit models (ECMs) [27]. ECMs are favored due to their simple architecture, minimal processing requirements, and real-time application, emulating battery behavior with fundamental electrical components like resistors and capacitors to provide precise SOC estimates. This paper emphasizes ECMs for their equilibrium between precision and simplicity of implementation. These models necessitate parameter identification customized for particular battery circumstances, accomplished by either offline or online tuning [28]. Offline approaches are typically preferred due to their simplicity and reduced computing expense, albeit they include a little trade-off in real-time precision. Contemporary SOC estimate strategies often depend on filtering mechanisms and state observers. Designing effective state observers is tough due to intricate convergence criteria that can impact estimation accuracy.

Among filtering methodologies, the Kalman filter (KF) family is particularly productive, diminishing sensor noise and providing high SOC precision with little computational complexity [29, 30]. The practicality of KF approaches renders them more advantageous than state observers in numerous applications. KF techniques enhance system parameters by leveraging data characteristics and the least squares principle [31], minimizing dependence on initial integration values [32] and obviating the necessity for large datasets, thus facilitating real-time SOC estimates [33]. Notwithstanding these benefits, conventional KF approaches face challenges with nonlinear and intricate dynamics [34]. The extended Kalman filter (EKF) is implemented to resolve this issue. The EKF technique improves linearization accuracy by using a high-order Taylor series expansion to approximate nonlinear OCV and SOC functions more precisely. Simplified Jacobian matrix approximations and sparse matrix approaches focus on crucial data points, reducing computing complexity while maintaining precision. Real-time modifications to model parameters, together with dynamic noise compensation, help sustain robust performance in quickly changing situations, further decreasing linearization faults. These strategies improve the EKF's capacity to address nonlinear dynamics. The main contributions of this paper can be effectively summarized as follows:

- Proposed an innovative SOC estimation method

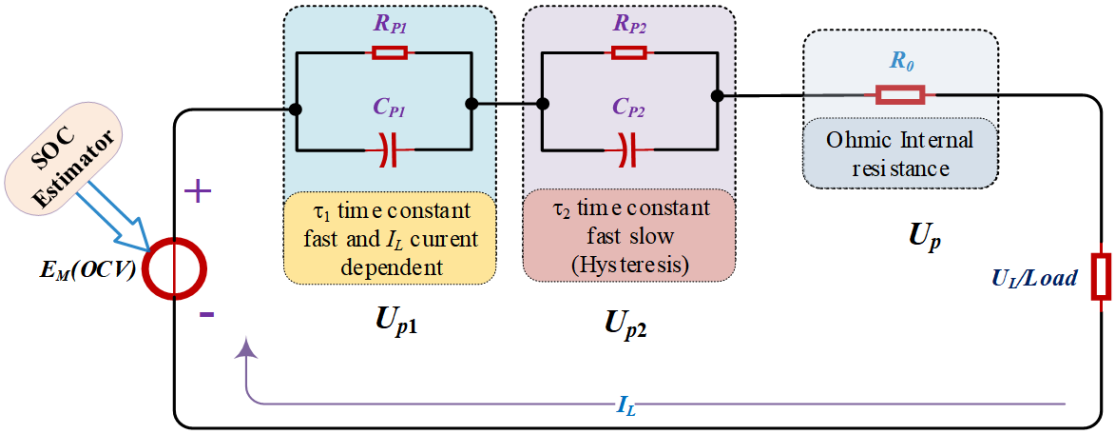

Figure 1. Proposed dynamic high-order ECM battery model.

for LIBs that integrates a dynamic high-order ECM with the EKF algorithm to enhance performance.

- Addressed model discrepancies and measurement uncertainties by accurately estimating noise variance and system states, achieving robust SOC predictions.
- Validated the superior accuracy, convergence rate, and resilience of the EKF algorithm through comprehensive testing under varied conditions, maintaining a minimal SOC estimation error within a range of 2.64% to -2.23%, even in challenging scenarios.

The structure of this paper is as follows: Section 2 provides a comprehensive mathematical analysis of SOC estimation, the dynamic high-order battery model, the impact of cell balancing on LIB performance, and the EKF algorithm. Section 3 details the experimental and results analysis, covering platform configuration, HPPC test performance, parameter identification, OCV testing, dynamic high-order model verification, and SOC estimation results. Finally, Section 4 presents the conclusion.

2 Mathematical Analysis

2.1 Definition of SOC

The SOC is a measure that indicates the remaining capacity of a battery expressed as a percentage of its total capacity. It is defined as the ratio of the battery current charge to its total capacity, reflecting the proportion of stored energy relative to its maximum potential [35]. A SOC of 100% denotes a fully charged battery, whereas a SOC of 0% represents a completely discharged condition. This statistic is essential for applications necessitating accurate energy management, such as EVs and portable gadgets, as it facilitates the monitoring and optimization of the battery's residual energy. The fundamental equation for SOC at any given time t is expressed as:

$$SOC(t) = \frac{1}{C_{nom}} \int_{t0}^{t} I(\tau)d\tau + SOC(t_0) \qquad (1)$$

In this context, $SOC(t)$ denotes the SOC at a given time t, while $SOC(t_0)$ represents the initial state at starting time t_0. C_{nom} is the nominal capacity of the battery, measured in AH. The current at any time τ is represented by $I(\tau)$, with discharge currents being negative and charge currents positive. The term $\int_{t0}^{t} I(\tau)d\tau$ reflects the integral of current over time, indicating the net charge added to or removed from the battery since time t_0. It is noted that this equation assumes ideal conditions, meaning real-world factors such as battery degradation, temperature, and self-discharge could impact the accuracy of SOC estimation.

2.2 Dynamic High-order Battery Model

An effective model-based estimation approach relies heavily on selecting an appropriate battery model, with various electrical models available to accurately simulate battery characteristics, such as the Thermal model, the ECM, and the electrochemical model. ECMs, widely used for replicating batteries dynamic behavior and voltage response under different current states, include types like the PNGV (Partnership for a New Generation of Vehicles) model, Rint model [36], GNL model, Thevenin model, and improved Thevenin model [37]. These models are built from basic circuit elements voltage sources, resistors, and capacitors and often employ an enhanced RC network for improved accuracy and structural integrity. This study employs an analogous circuit model with an extended two-RC

network, incorporating a resistor R0, two RC networks, and a voltage source Uoc, as illustrated in Figure 1.

The circuit model configuration is suitable for representing a two-state system. In this model, R_0 represents the ohmic internal resistance of the LIB. The elements R_{p1} and C_{p1} correspond to the electrochemical polarization resistance and capacitance, respectively, while R_{p2} and C_{p2} represent the resistance and capacitance associated with concentration polarization. The output voltage source U_{oc} maintains a consistent relationship with the SOC, and I_L denotes the charge current, with U_L representing the terminal voltage. Based on the behavior of dynamic high-order RC batteries, the voltage can be calculated as shown in Eq. (2).

$$U_L = E_m(OCV) - U_p - U_{p1} - U_{p2} \tag{2}$$

This study develops a model for LIBs in EVs, focusing on three key aspects: the electrical model, the thermal model, and the degradation model. In this framework, U_{p1}, U_{p2}, and the SOC are used as state variables, with U_L as the observation vector. The equivalent circuit model is represented by Eq.(3):

$$\begin{cases} U_{p1} = \dfrac{I_L}{C_{p1}} - \dfrac{U_{p1}}{C_{p1}R_{p1}} \\ U_{p2} = \dfrac{I_L}{C_{p2}} - \dfrac{U_{p2}}{C_{p2}R_{p2}} \end{cases} \tag{3}$$

The SOC vector represents the open-circuit voltage, establishing a non-linear relationship within the model. By applying concepts from current control theory, the circuit model can be discretized. For dynamic high-order ECMs, the selected state variables are [SOC, U_{p1}, U_{p2}]. The model's state-space representation, along with the SOC description, is further detailed in Eq. (4).

$$\begin{cases} \begin{bmatrix} SOC_{k+1} \\ U_{p1,k+1} \\ U_{p2,k+1} \end{bmatrix} = \begin{bmatrix} 1 & 0 & 0 \\ 0 & e^{-\frac{t}{\tau_{p1}}} & 0 \\ 0 & 0 & e^{-\frac{t}{\tau_{p2}}} \end{bmatrix} \begin{bmatrix} SOC_k \\ U_{p1,k} \\ U_{p2,k} \end{bmatrix} + \begin{bmatrix} -\frac{t}{\eta Q_0} \\ R_{p1}\left(1 - e^{-\frac{t}{\tau_{p1}}}\right) \\ R_{p2}\left(1 - e^{-\frac{t}{\tau_{p2}}}\right) \end{bmatrix} I(k) \\ U_{k+1} = U_{oc}(SOC_{k+1}) - U_{p1,k+1} - U_{p2,k+1} - iR_o \end{cases} \tag{4}$$

In Eq. (4), the model can be adapted for the recursive least-squares method, which enables efficient estimation of key parameters. This method yields the circuit modeling parameters R_0, R_{p1}, R_{p2}, C_{p1}, and C_{p2} derived from the identification results, thereby delivering a comprehensive depiction of the battery dynamic behavior. Utilizing recursive least squares, the model can perpetually enhance parameter values in real-time, hence augmenting its precision in representing the battery status across varying settings. This versatility is essential for applications requiring continuous status monitoring and accurate model modifications, such as EVs and various energy storage systems.

2.3 Impact of Cell Balancing on LIB Performance

Cell balance is critical for the performance, safety, and lifespan of LIB packs. These packs are made up of numerous cells connected in series or parallel, each with a somewhat different capacity, internal resistance, and SOC [38]. Over time, these variations might cause imbalances that harm the battery system. Cell balancing corrects these inequalities, maintaining consistent cell behavior and improving overall performance. The following is an analysis of the main impacts of cell balancing:

I Enhanced SOC accuracy:
Cell balancing ensures that the SOC is uniform across all cells, which improves the BMS accuracy in predicting the overall SOC [39]. Imbalances can cause cells to become under or overcharged, resulting in mistakes in SOC estimates. These inconsistencies impair energy efficiency, degrade performance, and jeopardize battery reliability. Balancing optimizes energy utilization and improves system reliability by equalizing SOC among cells.

II Prolonged battery lifespan:
Cell balancing increases battery life by correcting imbalances that cause rapid degradation. Without balancing, overcharging or deep draining individual cells causes premature breakdown and reduces battery life. Balancing prevents these extreme situations by maintaining regular charge levels, minimizing stress on individual cells, and guaranteeing consistent aging, all of which improve durability and long-term performance.

III Improved safety and thermal stability:
Cell balance is critical for assuring safety and thermal stability in LIB packs. Imbalances can cause overcharging or excessive discharging, which generates heat and increases the risk of thermal runaway, fires, and explosions [40]. Proper balance keeps cells within safe working limits, which prevents overheating and reduces these dangers. This increases safety while

charging and discharging and provides consistent, stable performance under changing situations.

2.4 The Mechanism of the EKF Algorithm

The KF is a robust technique designed to estimate a system's present state with a linear state-space model, incorporating system inputs and outputs. Although the classic KF is best for linear systems, numerous actual applications, such as assessing the SOC in LIBs, are fundamentally non-linear. The EKF modifies the KF for non-linear systems [41]. The EKF approximates non-linear state-space equations by employing a first-order Taylor series expansion, enabling successful estimation of the current state without necessitating full linearity [42, 43].

In this process, the EKF retains only the first-order terms from the Taylor expansion, discarding higher-order terms to approximate local linear behavior [44]. This adaptation enables the EKF to apply the KF to the locally linearized model, producing a near-optimal state estimate. It is particularly effective for discrete-time non-linear systems that require precise real-time state estimation. The EKF operates in two primary phases: the Prediction Phase and the Update (Correction) Phase.

2.4.1 Prediction Phase

In this phase, the EKF uses the current state estimate to predict the next state and its associated error covariance.

I. State Prediction:

$$\hat{x}_k|_{k-1} = f(\hat{x}_{k-1}|_{k-1}, u_{k-1}) \tag{5}$$

where, $\hat{x}_k|_{k-1}$ represents the predicted state at time k, based on the previous state estimate $\hat{x}_{k-1}|_{k-1}$ and the control input U_{k-1}. The function f models the non-linear dynamics of the system, allowing for the projection of the state forward in time based on past state estimates, independent of new measurements.

II. Jacobian of the State Transition Model:

$$F_{k-1} = \frac{\partial f}{\partial x}\bigg|\hat{x}_{k-1}|_{k-1}, u_{k-1} \tag{6}$$

Given the non-linearity of f, it is linearized around the previous state estimate $\hat{x}_{k-1}|_{k-1}$ using its Jacobian, F_{k-1}. This matrix of partial derivatives of f with respect to x enables the use of the KF framework, initially designed for linear systems.

III. Covariance Prediction:

$$P_{k|k-1} = F_{k-1}P_{k-1|k-1}F_{k-1}^T + Q_{k-1} \tag{7}$$

The predicted error covariance $P_{k|k-1}$ quantifies the uncertainty in the state prediction by combining the previous error covariance $P_{k-1|k-1}$, the Jacobian F_{k-1}, and the process noise covariance Q_{k-1}. This step updates the uncertainty associated with the state estimate as it propagates through the non-linear dynamics.

2.4.2 Update (Correction) Phase

The update phase refines the state prediction by incorporating a new measurement, thus enhancing accuracy.

I. Measurement Prediction:

$$\hat{z}_{k|k-1} = h(\hat{x}_{k|k-1}) \tag{8}$$

where, $\hat{z}_{k|k-1}$ represents the predicted measurement, obtained by applying the non-linear observation function h to the predicted state $\hat{x}_{k|k-1}$. This step enables comparison with the actual measurement z_k.

II. Jacobian of the Observation Model:

$$H_k = \frac{\partial h}{\partial x}\bigg|\hat{x}_k|_{k-1} \tag{9}$$

Like f, the observation function h is non-linear, so it is linearized around the predicted state $\hat{x}_{k|k-1}$. The Jacobian H_k is the matrix of partial derivatives of h with respect to x, evaluated at $\hat{x}_{k|k-1}$, which transforms the state covariance into measurement space for Kalman gain calculation.

III. Innovation (Residual):

$$y_k = z_k - \hat{z}_{k|k-1} \tag{10}$$

The innovation y_k represents the difference between the actual measurement z_k and the predicted measurement $\hat{z}_{k|k-1}$, indicating the error in the prediction. This residual guides the correction applied to the state estimate.

IV. Innovation Covariance:

$$S_k = H_kP_{k|k-1}H_k^T + R_k \tag{11}$$

The innovation covariance S_k reflects the uncertainty in the innovation y_k, combining the projected error covariance in the measurement space $H_kP_{k|k-1}H_k^T$ with the measurement noise covariance R_k. A higher

S_k implies greater uncertainty, influencing the Kalman gain.

V. Kalman Gain:

$$K_k = P_{k|k-1} H_k^T S_k^{-1} \tag{12}$$

The Kalman gain K_k determines the weight given to the measurement in updating the state estimate, balancing the predicted state and the new measurement based on their uncertainties. A higher Kalman gain favors the measurement, while a lower gain favors the prediction.

VI. State Update:

$$\hat{x}_{k|k} = \hat{x}_{k|k-1} + K_k y_k \tag{13}$$

The updated state $\hat{x}_{k|k}$ is obtained by adjusting the predicted state $\hat{x}_{k|k-1}$ with the innovation y_k scaled by the Kalman gain K_k, incorporating new information to refine the state estimate.

VII. Covariance Update:

$$P_{k|k} = (I - K_k H_k) P_{k|k-1} \tag{14}$$

Finally, the error covariance $P_{k|k}$ is updated to reflect reduced uncertainty after incorporating the new measurement, resulting in a more precise estimate.

3 Experiments and Results Analysis

3.1 Experiment Platform Setup

The battery test platform used in this experiment is equipped with Shenzhen Xinwei New Energy Technology Corporation's CT-4616-5V100A-NTFA equipment. This platform, shown in Figure 2, enables precise charging and discharging of a ternary LIB module, with a maximum input voltage of 380V at 50/60Hz and a peak current of 100 A. The system is intended for high-performance battery testing, enabling extensive investigation of battery behavior under a variety of settings. Key parameters like voltage, current, and temperature are detected and recorded in real-time on a host computer running the BTS-7.6 software. This program, with its extensive data-gathering capabilities, sends important performance data to the main control system over TCP/IP, allowing for continuous monitoring and control during the testing process.

To maintain consistent environmental conditions, the battery testing is conducted within a temperature-controlled chamber (model DGBELL-BTT-331C), which can regulate both high and low temperatures, ensuring a steady 25°C throughout the tests. The testing setup includes components such as a CAN unit, battery management system (BMS), and LIB modules, all interconnected through power and data lines for seamless monitoring. The specifications of the battery, including dimensions, rated voltage, and operating temperature, are detailed in Table 1. The experiment is designed to assess the battery actual discharge capacity under varying conditions, considering potential capacity degradation due to factors like recycling. This calibration and evaluation are crucial for accurate SOC assessments during battery operations.

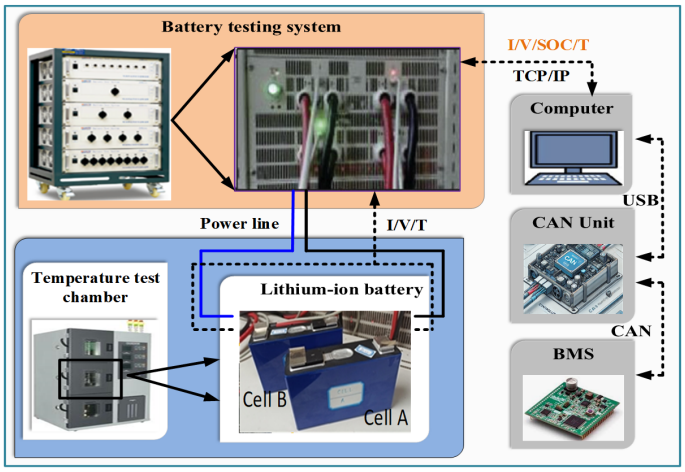

Figure 2. Experimental platform setup procedure.

Table 1. Key function of battery parameters.

Criteria	Parameters
Working temperature/°C	25
The discharge cutoff voltage/V	2.60
Size: length*width*height/mm	200*80*180
The charge cut off voltage/V	4.20
Rated Voltage	3.80
Maximum Load current/A	70

3.2 HPPC Test Performance

The hybrid pulse power characterization (HPPC) test is a fundamental technique for evaluating battery performance, serving as the foundation for examining power behavior and determining critical parameters in battery models. This assessment delineates offline factors and is extensively utilized. The HPPC test comprises a series of profiles that alternate between constant current discharge pulses and rest intervals, facilitating a comprehensive assessment of a battery's dynamic reactions. Created by the Idaho National Engineering and Environmental Laboratory (INEEL) as part of the Freedom CAR energy storage effort,

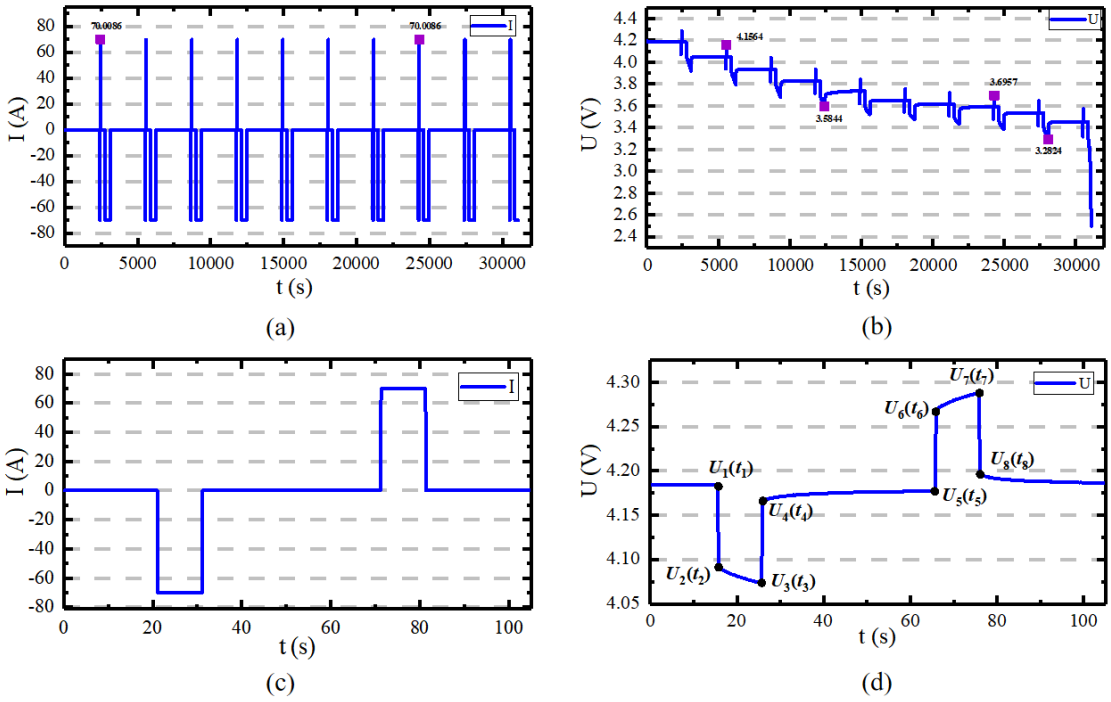

Figure 3. Complete and single current-voltage results: (a) Complete HPPC current curve, (b) Complete HPPC voltage curve, (c) Single HPPC current curve, (d) Single HPPC voltage curve.

this test delineates battery power characteristics across diverse situations. In addition to performance analysis, the HPPC test facilitates the configuration of circuit module characteristics to align with battery standards. Figure 3(a) and 3(b) illustrate the current and voltage profiles of a whole HPPC test cycle, whereas Figure 3(c) and 3(d) present individual current and voltage curves. Using batteries of identical capacity and origin ensures consistency, reducing variations and focusing on experimental conditions.

The discharge process follows a specific sequence:

1. At time t_1, the discharge begins, causing a sharp drop in terminal voltage from U_1 to U_2 due to the LIB internal resistance.
2. From t_2 to t_3, the voltage gradually decreases from U_2 to U_3, influenced by battery polarization and the RC circuit's zero-state response.
3. Between t_3 and t_4, a sudden voltage increase from U_3 to U_4 occurs, attributed to shifts in the battery's internal resistance.
4. Finally, between t_4 and t_5, the terminal voltage rises steadily from U_4 to U_5 as the polarization capacitance discharges, demonstrating the RC circuit's zero response.

Figure 3(d) illustrates the variable and stable behaviors of the LIB, with each voltage measurement adhering to particular requirements, hence proving meticulous monitoring of voltage and current under regulated conditions.

3.3 Parameter Identification

Parameter identification in LIBs is essential for comprehending the internal properties and behaviors that affect a battery performance, efficiency, and safety. This entails estimating critical parameters such as internal resistance, SOC, state of health, capacity degradation, and thermal dynamics. These factors are crucial for precise modeling and simulation, facilitating the creation of resilient BMS that oversee and enhance battery performance in real time. This investigation determined that online parameter detection would elevate computational complexity without enhancing accuracy; thus, offline identification was selected. At 25°C, the battery was subjected to an HPPC test, facilitating the extraction of model parameters through the analysis of the battery's operating characteristics. Table 2 shows the findings of the identified parameters, based on HPPC data at each point, and provides values for the dynamic high-order ECM parameters at various SOC levels.

With this method, researchers can forecast battery life, assess deterioration, and improve LIBs flexibility for uses such as renewable energy storage and electric cars. The HPPC test at 25°C revealed important

Table 2. Parameter identification at different SOC levels.

SOC (%)	*OCV*/*V*	R_0/Ω	R_{P1}/Ω	R_{P2}/Ω	C_{P1}/F	C_{P2}/F
10	3.4545	0.00151	0.0007	0.0001	17539.6664	4414.2351
20	3.5368	0.00141	0.0005	0.0000	27581.6998	12980.6094
30	3.5900	0.00142	0.0004	0.0000	31625.7092	18372.8397
40	3.6166	0.00131	0.0004	0.0000	37939.8988	32882.0200
50	3.6512	0.00132	0.0006	0.0000	31707.6273	19733.8402
60	3.7363	0.00131	0.0003	0.0000	24409.4122	18973.3658
70	3.8309	0.00134	0.0006	0.0000	23566.6671	20541.1868
80	3.9362	0.00133	0.0004	0.0001	25101.4887	93120.7288
90	4.0515	0.00131	0.0005	0.0000	26116.6477	19737.7047
100	4.1845	0.00132	0.0004	0.0000	26421.0526	116563.8765

characteristics necessary for a precise evaluation of battery performance. The findings, which are displayed in Table 2, support accurate modeling and the creation of sophisticated BMS to track and improve battery performance in real time by providing dynamic high-order ECM parameter values across SOC levels.

3.4 Open Circuit Voltage Test

The OCV test is a crucial diagnostic technique for evaluating the health and SOC of LIBs. In this test, the battery is permitted to rest in an open-circuit condition, detached from any external load, to allow the voltage to settle. The measured OCV, obtained in the absence of current flow, indicates the battery SOC as it signifies the equilibrium potential resulting from internal electrochemical reactions. This investigation involved the collection of OCV-SOC data points to construct a curve illustrating the correlation between OCV and SOC, as depicted in Figure 4. The plot demonstrates an ascending trend in OCV as SOC increases, exhibiting a steeper slope at elevated SOC values, signifying a non-linear connection. This curve was produced via a curve-fitting method, yielding a precise representation of OCV behavior across various SOC levels. The non-invasive characteristics of OCV testing provide significant insights into battery status without depleting or modifying the battery's state. This renders it an essential instrument for BMS to assess SOC, detect aging effects, and identify potential problems. An established OCV-SOC model facilitates ongoing assessment of battery performance and assists in predicting battery lifespan, hence aiding applications like EVs and renewable energy storage systems.

The non-invasive characteristics of OCV testing provide significant insights into battery status without depleting or modifying the battery's state. This renders it an essential instrument for BMS to assess SOC, detect aging effects, and identify potential problems. An established OCV-SOC model facilitates ongoing assessment of battery performance and assists in predicting battery lifespan, benefiting applications such as EVs and renewable energy storage systems.

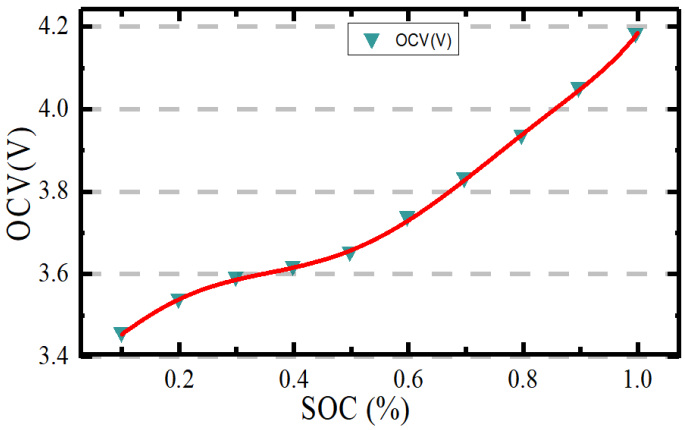

Figure 4. The SOC-OCV relationship curve.

3.5 The Dynamic High-order Model Verification Approach

The dynamic high-order model validation technique utilizes an ordinary differential equation framework to mimic the ECM in the temporal domain. Utilizing Simulink, the model voltage response is discretized, facilitating a discrete state-space formulation crucial for dynamic high-order models. The model emphasizes several electrical factors, including current I, internal resistance R_0, polarization resistances R_{p1} and R_{p2}, and polarization capacitors C_{p1} and C_{p2}. These characteristics are augmented by open-circuit voltage U_{oc}, terminal voltage U_L, and load current I_L. The model includes internal parameters that change dynamically to the SOC, seen as an independent variable. As the SOC evolves, the model utilizes historical states to preserve a connection with the present charge state, considering recent variations.

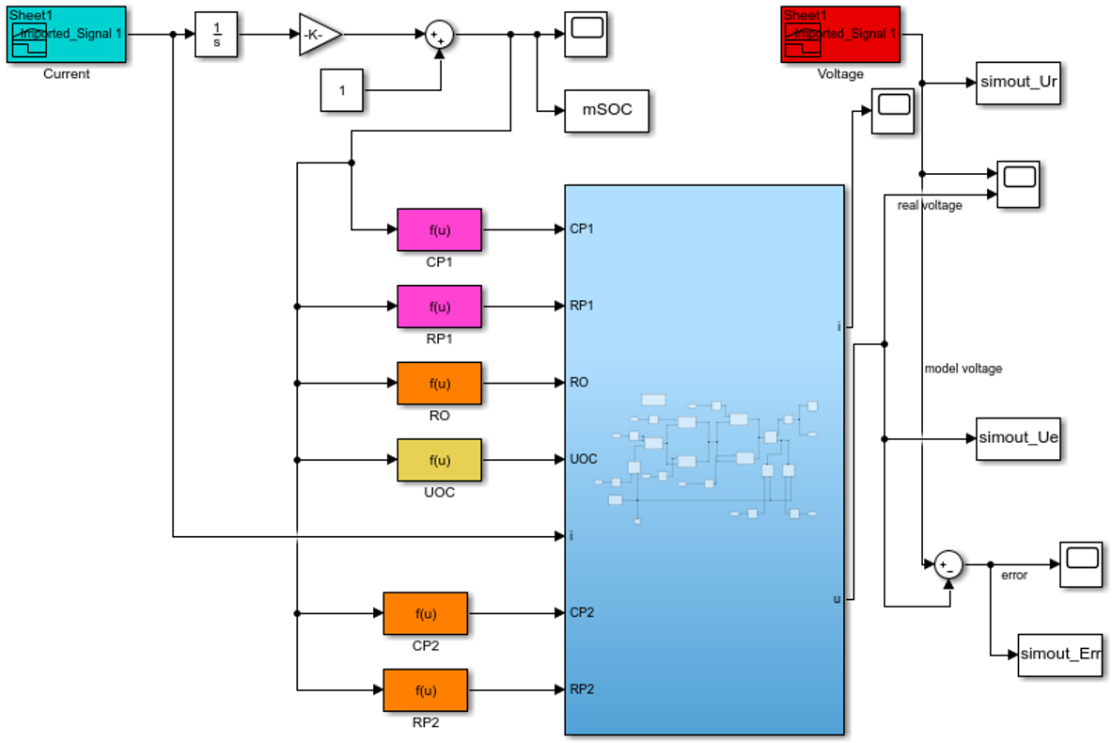

Figure 5. The verification structure of the dynamic high-order ECM in Simulink.

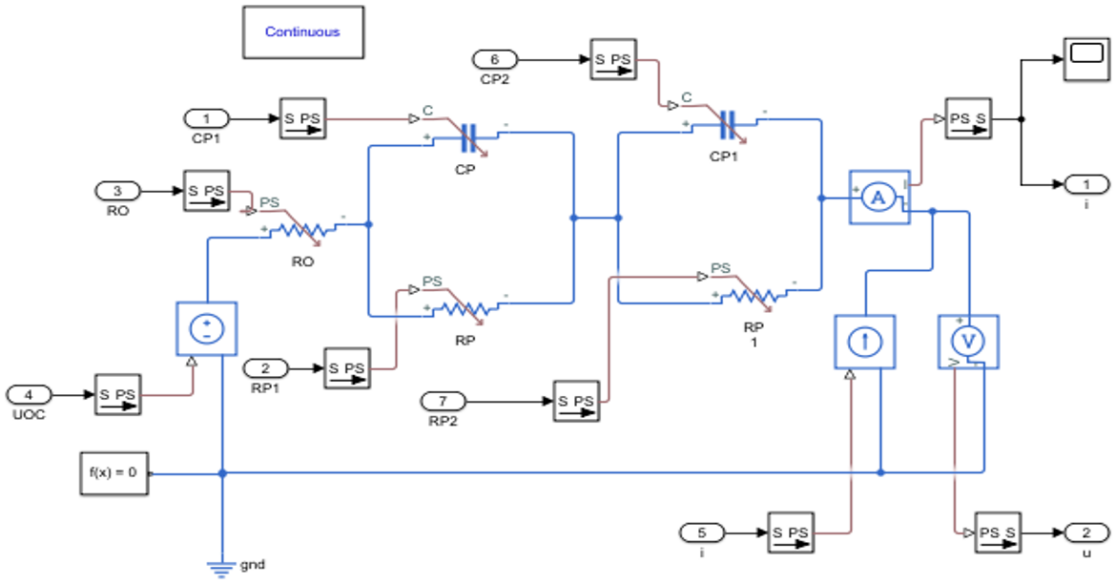

Figure 6. Internal Structure of the Dynamic High-Order ECM.

Figure 5 presents a Simulink simulation comparing actual and simulated voltage responses to evaluate the accuracy, with error indicators and metrics validating the model performance and reliability in capturing real-time voltage dynamics.

The configuration comprises adjustable voltage and current sources that engage via signal interfaces, transforming electrical inputs into signals that actuate the model. External voltage and current sensors operate as transducers, enabling seamless integration inside the circuit model. This design facilitates accurate monitoring and control, guaranteeing that the dynamic high-order model precisely represents real-time operational characteristics.

Figure 6 depicts the operational mechanisms of the dynamic high-order ECM, wherein each circuit component evolves over time to accommodate changing situations. This model consists of seven primary inputs: I_L, R_0, R_{p1}, R_{p2}, C_{p1}, C_{p2}, and U_{oc}, which collectively regulate U_L under varying

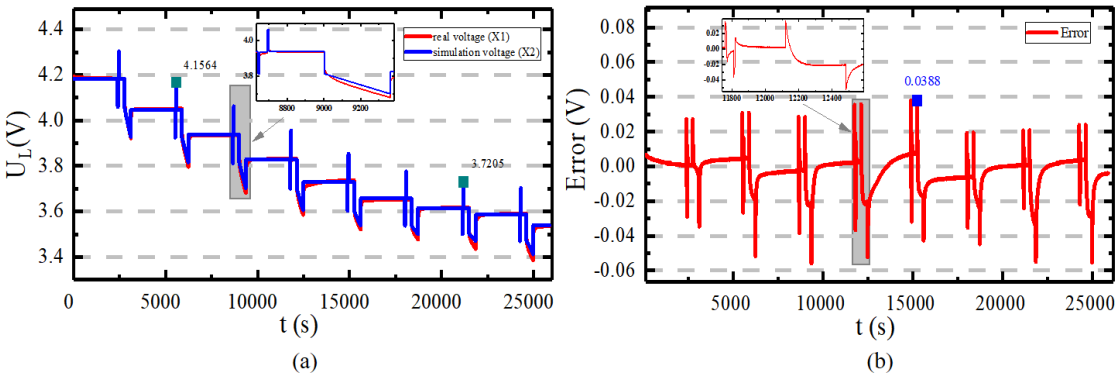

Figure 7. High-order simulation model verification and experimental error curve: (a) high-order voltage variation curve, (b) high-order simulation error indication curve.

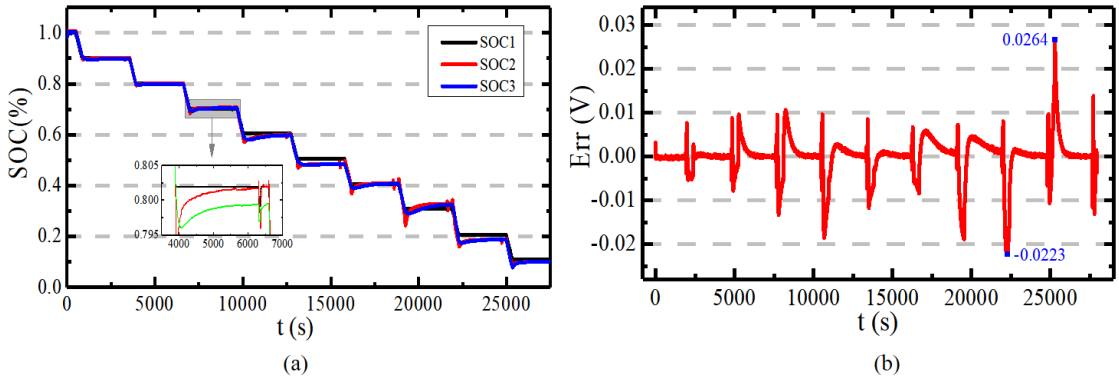

Figure 8. SOC estimation verification results using the EKF algorithm: (a) EKF-SOC estimation simulation result, (b) SOC estimation error curve.

conditions. To validate the dynamic high-order ECM, real voltage and current data from cyclic discharge tests are imported into a MATLAB/Simulink-based simulation. This model replicates battery behavior across different SOC states. SOC values are dynamically measured and linked to a function correlating SOC and U_{oc}, enabling tracking of the battery voltage over time. In this approach, U_{oc} is integrated into the model to calculate the battery terminal voltage, which is then compared to actual terminal voltage measurements.

Figure 7 presents the verification of the high-order simulation model along with the corresponding experimental error curve. The solid blue line (X2) represents the estimated output voltage derived from the model, while the solid red line (X1) indicates the real battery terminal voltage. The close alignment between the model output voltage and the real measurements demonstrates the reliability and effectiveness of the parameter identification method, as illustrated in Figure 7 (a).

Figure 7(b) also illustrates the simulation error. The difference between the estimated output voltage and the actual battery terminal voltage, referred to as the model error, highlights the impact of simulation accuracy on the results. The mean-variance is roughly 3.88%, potentially indicating the battery performance during pivotal moments during discharge. Error study reveals that discrepancies in voltage estimations typically escalate towards the conclusion of the battery discharge cycle. This indicates a substantial alteration in battery voltage as it nears the concluding stage of discharge, highlighting the want for accurate modeling. Notwithstanding these slight inaccuracies, the simulation model attains an exceptional accuracy rate of 99.15%, with the maximum recorded voltage of the LIB reaching 4.2V.

3.6 Verification of SOC Estimation Results for the EKF Algorithm

To assess the efficacy of the EKF algorithm, a dynamic high-order ECM was carefully calibrated by adjusting parameters derived from HPPC testing. This calibration is essential for synchronizing the model's behavior with the true dynamics of the battery. After calibration, the model's output undergoes a rigorous comparison with actual battery data to verify its accuracy. The model simulates continuous battery discharge over a specified

duration, accurately capturing a range of real-world operating conditions, and making it suitable for practical applications. During this validation process, up-to-date experimental data is used as input for the model, and the simulated terminal voltage is compared to the measured values, as shown in Figure 8.

Figure 8(a) shows the SOC estimation results for three methods: SOC1 as the genuine SOC, SOC2 calculated using a standard ECM with an EKF, and SOC3 estimated using a dynamic high-order ECM with an EKF. Figure 8(b) illustrates the error curve, with the red line showing the deviation between the EKF's SOC estimate and the actual SOC from test data. The results show that the EKF algorithm greatly decreases the initial SOC estimation error, attaining high robustness with an error margin of less than 2.64% under steady conditions. This precision demonstrates the EKF dependability in providing correct SOC estimates under different situations, highlighting its applicability for real-time BMS. Furthermore, the suggested filter accurately reflects the system's real-world dynamics. Overall, the experiment confirms that the EKF algorithm provides consistent, precise SOC estimates for LIBs.

4 Conclusion

This research employs a dynamic high-order ECM to accurately identify parameters for LIBs. Through rigorous circuit analysis, exact expressions for the 2RC time constant and terminal voltage are derived. Using EKF algorithms based on HPPC tests, precise parameter identification is achieved, followed by the construction of a MATLAB Simulink model to validate the findings against HPPC experimental data. The developed parameter identification method demonstrates over 98.16% accuracy for the ECM. This work presents a reliable approach for LIB parameter identification, establishing a critical foundation for SOC estimation in BMS. Additionally, by applying linearization techniques, the study constructs a dynamic high-order ECM and implements an EKF for SOC estimation. The efficacy of the algorithm is experimentally validated through battery discharge tests on both fully and partially charged batteries, with an error margin of less than 2.64%. The proposed algorithm's effectiveness is further confirmed through experiments on both fully and partially discharged batteries, establishing its practical reliability. However, despite its potential to significantly advance battery development, the proposed method has a notable limitation: it is susceptible to the effects of aging and high temperatures, which degrade the accuracy of SOC estimation and, consequently, reduce its overall effectiveness. This limitation highlights the need for future research into more sophisticated strategies, particularly those based on machine learning, to address these challenges.

Data Availability Statement

Data will be made available on request.

Funding

This work was supported in part by the National Natural Science Foundation of China under Grant 62373256, the Guangdong Basic and Applied Research Foundation under Grant 2024A1515013154 and the Science and Technology Development Foundation of the Shenzhen Government under Grant JCYJ20240813141419025.

Conflicts of Interest

The authors declare no conflicts of interest.

Ethical Approval and Consent to Participate

Not applicable.

References

[1] Hou, J., et al. (2023). Robust lithium-ion state-of-charge and battery parameters joint estimation based on an enhanced adaptive unscented Kalman filter. *Energy*, 271, 126998. [CrossRef]

[2] Chang, C., Wang, S., Tao, C., Jiang, J., Jiang, Y., & Wang, L. (2022). An improvement of equivalent circuit model for state of health estimation of lithium-ion batteries based on mid-frequency and low-frequency electrochemical impedance spectroscopy. *Measurement*, 202, 111795. [CrossRef]

[3] Li, H., Wang, S., Islam, M., Bobobee, E. D., Zou, C., & Fernandez, C. (2022). A novel state of charge estimation method of lithium-ion batteries based on the IWOA-AdaBoost-Elman algorithm. *International Journal of Energy Research*, 46(4), 5134-5151. [CrossRef]

[4] Zeng, X., et al. (2019). Commercialization of Lithium Battery Technologies for Electric Vehicles. *Advanced Energy Materials*, 9(27), 1900161. [CrossRef]

[5] Qiu, L., Wen, Y., Monirul, I. M., Najariyan, M., Pan, J., & Wu, Z. (2024). Networked H∞ Control and its Applications for a Multi-Station Cooperative Motion System. *IEEE Transactions on Automation Science and Engineering*, 21(4), 7107-7116. [CrossRef]

[6] Qiu, L., Yu, J., Monirul, I. M., Liu, C., & Wu, Z. (2023). Consensus control of semi-Markov jump topology multiple direct-drive motion system. *IET Control Theory & Applications*, 17(15), 2071-2084. [CrossRef]

[7] Monirul, I. M., Qiu, L., & Ruby, R. (2025). Accurate state of charge estimation for UAV-centric lithium-ion batteries using customized unscented Kalman filter. *Journal of Energy Storage*, 107, 114955. [CrossRef]

[8] How, D. N. T., Hannan, M. A., Lipu, M. S. H., & Ker, P. J. (2019). State of Charge Estimation for Lithium-Ion Batteries Using Model-Based and Data-Driven Methods: A Review. *IEEE Access*, 7, 136116-136136. [CrossRef]

[9] Elsanhoury, M., Koljonen, J., Elmusrati, M., & Niemi, S. (2024, December). State of Charge Estimation for Lithium-Ion Batteries in Hybrid Vessels Using Kalman Filters. In *2024 25th International Middle East Power System Conference (MEPCON)* (pp. 1-6). IEEE. [CrossRef]

[10] Guo, S., & Ma, L. (2023). A comparative study of different deep learning algorithms for lithium-ion batteries on state-of-charge estimation. *Energy*, 263, 125872. [CrossRef]

[11] Sharafian, A., & Ghasemi, R. (2019). Fractional neural observer design for a class of nonlinear fractional chaotic systems. *Neural Computing and Applications*, 31(4), 1201-1213. [CrossRef]

[12] Liu, Z., Dang, X., & Jing, B. (2019). A novel open circuit voltage based state of charge estimation for lithium-ion battery by multi-innovation Kalman filter. *IEEE Access*, 7, 49432-49447. [CrossRef]

[13] Zhang, X., Duan, L., Gong, Q., Wang, Y., & Song, H. (2024). State of charge estimation for lithium-ion battery based on adaptive extended Kalman filter with improved residual covariance matrix estimator. *Journal of Power Sources*, 589, 233758. [CrossRef]

[14] Duan, L., Zhang, X., Jiang, Z., Gong, Q., Wang, Y., & Ao, X. (2023). State of charge estimation of lithium-ion batteries based on second-order adaptive extended Kalman filter with correspondence analysis. *Energy*, 280, 128159. [CrossRef]

[15] Peng, S., Zhang, A., Liu, D., Cheng, M., Kan, J., & Pecht, M. (2023). State-of-charge estimation of lithium-ion batteries based on dual-coefficient tracking improved square-root unscented Kalman filter. *Batteries*, 9(8), 392. [CrossRef]

[16] Li, H., Fu, L., Long, X., Liu, L., & Zeng, Z. (2024). A hybrid deep learning model for lithium-ion batteries state of charge estimation based on quantile regression and attention. *Energy*, 294, 130834. [CrossRef]

[17] Xiong, R., et al. (2023). Co-Estimation of State-of-Charge and State-of-Health for High-Capacity Lithium-Ion Batteries. *Batteries*, 9(10), 509. [CrossRef]

[18] Qiu, H., Korovin, I., Liu, H., Gorbachev, S., Gorbacheva, N., & Cao, J. (2024). Distributed adaptive neural network consensus control of fractional-order multi-agent systems with unknown control directions. *Information Sciences*, 655, 119871. [CrossRef]

[19] Wei, M., Ye, M., Zhang, C., Lian, G., Xia, B., & Wang, Q. (2024). Robust state of charge estimation of LiFePO4 batteries based on Sage_Husa adaptive Kalman filter and dynamic neural network. *Electrochimica Acta*, 477, 143778. [CrossRef]

[20] He, L., Hu, X., Yin, G., Shao, X., Liu, J., & Shi, Q. (2023). A voltage dynamics model of lithium-ion battery for state-of-charge estimation by proportional-integral observer. *Applied Energy*, 351, 121793. [CrossRef]

[21] Mohammadi, H., & Karwowski, W. (2024). Graph Neural Networks in Brain Connectivity Studies: Methods, Challenges, and Future Directions. *Brain Sciences*, 15(1), 17. [CrossRef]

[22] Sharafian, A., Sharifi, A., & Zhang, W. (2020). Fractional sliding mode based on RBF neural network observer: Application to HIV infection mathematical model. *Computers & Mathematics with Applications*, 79(11), 3179-3188. [CrossRef]

[23] Sharafian, A., Bagheri, V., & Zhang, W. (2018). RBF Neural Network Sliding Mode Consensus of Multiagent Systems with Unknown Dynamical Model of Leader-follower Agents. *International Journal of Control, Automation and Systems*, 16(2), 749-758. [CrossRef]

[24] Geng, Y., Pang, H., & Liu, X. (2022). State-of-charge estimation for lithium-ion battery based on PNGV model and particle filter algorithm. *Journal of Power Electronics*, 22(7), 1154-1164. [CrossRef]

[25] Shi, Z., Bai, Y., Jin, X., Wang, X., Su, T., & Kong, J. (2021). Parallel deep prediction with covariance intersection fusion on non-stationary time series. *Knowledge-Based Systems*, 211, 106523. [CrossRef]

[26] Chaudhary, A. K., Roy, S., Guha, D., Negi, R., & Banerjee, S. (2024). Adaptive cyber-tolerant finite-time frequency control framework for renewable-integrated power system under deception and periodic denial-of-service attacks. *Energy*, 302, 131809. [CrossRef]

[27] Yu, H., et al. (2023). State of charge estimation method by using a simplified electrochemical model in deep learning framework for lithium-ion batteries. *Energy*, 278, 127846. [CrossRef]

[28] Yang, H., Sun, X., An, Y., Zhang, X., Wei, T., & Ma, Y. (2019). Online parameters identification and state of charge estimation for lithium-ion capacitor based on improved Cubature Kalman filter. *Journal of Energy Storage*, 24, 100810. [CrossRef]

[29] Fan, Y., Wang, S., Jiang, C., & Fernandez, C. (2021). The power state estimation method for high energy ternary lithium-ion batteries based on the online collaborative equivalent modeling and adaptive correction-unscented Kalman filter. *International journal of electrochemical science*, 16(1), 151020. [CrossRef]

[30] Zhuang, Y., Wang, Q., Shi, M., Cao, P., Qi, L., & Yang, J. (2019). Low-power centimeter-level localization for indoor mobile robots based on ensemble Kalman smoother using received signal strength. *IEEE Internet of Things Journal*, 6(4), 6513-6522. [CrossRef]

[31] Duan, J., Wang, P., Ma, W., Qiu, X., Tian, X., & Fang, S. (2020). State of charge estimation of lithium battery based on improved correntropy extended Kalman filter. *Energies*, 13(16), 4197. *Energies*, 13(16), 4197. [CrossRef]

[32] Choi, G., Park, J., Shlezinger, N., Eldar, Y. C., & Lee, N. (2023). Split-KalmanNet: A robust model-based deep learning approach for state estimation. *IEEE transactions on vehicular technology*, 72(9), 12326-12331. [CrossRef]

[33] Zafar, M. H., Bukhari, S. M. S., Abou Houran, M., Mansoor, M., Khan, N. M., & Sanfilippo, F. (2024). DeepTimeNet: A novel architecture for precise surface temperature estimation of lithium-ion batteries across diverse ambient conditions. *Case Studies in Thermal Engineering*, 61, 105002. [CrossRef]

[34] Pérez, G., Garmendia, M., Reynaud, J. F., Crego, J., & Viscarret, U. (2015). Enhanced closed loop State of Charge estimator for lithium-ion batteries based on Extended Kalman Filter. *Applied Energy*, 155, 834-845. [CrossRef]

[35] Yuan, B., et al. (2024). Study on the estimation of the state of charge of lithium-ion battery. *Electrochimica Acta*, 491, 144297. [CrossRef]

[36] Pu, R., Wang, S., Chen, X., Huang, J., He, M., & Cao, W. (2022). A novel cuckoo search particle filtering strategy for the remaining useful life prediction of the lithium-ion batteries in hybrid electric vehicle. *International Journal of Energy Research*, 46(15), 21703-21715. [CrossRef]

[37] Xiong, R., Wang, S., Yu, C., Fernandez, C., Xiao, W., & Jia, J. (2023). A novel nonlinear decreasing step-bacterial foraging optimization algorithm and simulated annealing-back propagation model for long-term battery state of health estimation. *Journal of Energy Storage*, 59, 106484. [CrossRef]

[38] Hoekstra, F. S. J., Bergveld, H. J., & Donkers, M. C. F. (2022). Optimal Control of Active Cell Balancing: Extending the Range and Useful Lifetime of a Battery Pack. *IEEE Transactions on Control Systems Technology*, 30(6), 2759-2766. [CrossRef]

[39] Ouyang, Q., Han, W., Zou, C., Xu, G., & Wang, Z. (2020). Cell Balancing Control For Lithium-Ion Battery Packs: A Hierarchical Optimal Approach. *IEEE Transactions on Industrial Informatics*, 16(8), 5065-5075. [CrossRef]

[40] Omariba, Z. B., Zhang, L., & Sun, D. (2019). Review of Battery Cell Balancing Methodologies for Optimizing Battery Pack Performance in Electric Vehicles. *IEEE Access*, 7, 129335-129352. [CrossRef]

[41] Zhang, F., Li, S., Yuan, S., Sun, E., & Zhao, L. (2017, July). Algorithms analysis of mobile robot SLAM based on Kalman and particle filter. In *2017 9th International Conference on Modelling, Identification and Control (ICMIC)* (pp. 1050-1055). IEEE. [CrossRef]

[42] Chen, X., Chen, X., & Chen, X. (2021). A novel framework for lithium-ion battery state of charge estimation based on Kalman filter Gaussian process regression. *International Journal of Energy Research*, 45(9), 13238-13249. [CrossRef]

[43] Gutmann, J. S., & Fox, D. (2002, September). An experimental comparison of localization methods continued. In *IEEE/RSJ International Conference on Intelligent Robots and Systems* (Vol. 1, pp. 454-459). IEEE. [CrossRef]

[44] Bahraini, M. S., Mahmoodabadi, M. J., & Lohse, N. (2023). Robust adaptive fuzzy fractional control for nonlinear chaotic systems with uncertainties. *Fractal and Fractional*, 7(6), 484. [CrossRef]

Islam Md Monirul received the M.E. degree in Information and Communication Engineering from the Southwest University of Science and Technology, Mianyang, China, in 2021. He is currently pursuing the Ph.D. degree in Optomechatronics Engineering and Applications with the College of Mechatronics and Control Engineering, Shenzhen University, Shenzhen, China. His research interests include battery modeling, lithium-ion batteries, energy storage system, renewable energy, networked control systems. (Email: islammdmonirul@email.szu.edu.cn)

Li Qiu (Member, IEEE) received the M.S. and Ph.D. degrees in control science and control engineering from the South China University of Technology, Guangzhou, China, in 2006 and 2011, respectively. From 2016 to 2017, she served as a Visiting Scholar at the Department of Mechanical Engineering, University of Victoria, Victoria, BC, Canada. Currently, she works as a Professor at the College of Mechatronics and Control Engineering, Shenzhen University, Shenzhen, China. Her research interests include networked motion control systems, artificial intelligence and intelligent control systems. (Email: qiuli@szu.edu.cn)

Inam Ullah received a B.Sc. degree in Electrical Engineering from the Department of Electrical Engineering, University of Science and Technology Bannu, Pakistan, in 2016 and a Master's and Ph.D. degree in Information and Communication Engineering from the College of Internet of Things Engineering, Hohai University, China, in 2018 and 2022, respectively. He completed his postdoc with BK21, Chungbuk National University, S Korea, in 2023. He is currently an Assistant Professor at the Department of Computer Engineering, Gachon University, S Korea. His research interests include Robotics, IoT, WSNs, AUVs, AI, Deep learning,

etc. He has authored more than 100 articles and five books as an editor. (Email: inam@gachon.ac.kr)

Khongorzul Dashdondov received her B.S. and M.S. degrees in mathematics from the School of Mathematics and Computer Science at the National University of Mongolia in 1998 and 2000, respectively. She earned her Ph.D. from the Mobile/Multimedia Communication Research Laboratory, Department of Radio and Communication Engineering, Chungbuk National University, South Korea in 2013. From 2017 to 2023, she was a Postdoctoral Research Fellow at the Ubiquitous Game Laboratory, Chungbuk National University. Since 2023, she has been an Assistant Professor in the Department of Computer Engineering at Gachon University, Seongnam. Her research interests include queuing theory, artificial intelligence, deep learning, big data analysis, and healthcare analytics. (Email: khongor@chungbuk.ac.kr)

Rehan Ali Khan received Ph.D. degree from the College of Electrical Engineering, Zhejiang University Hangzhou, P.R China in 2022. He did Masters in Electronics and Communication from the University Of Lahore, Pakistan, where Bachelor degree in Telecommunication Engineering from Balochistan University of Information Technology, Engineering and Management Sciences Quetta. He is working as an Assistant Professor at the Department of Electrical Engineering, University of Science & Technology Bannu, Pakistan since 2011. Research interest including Optimization, AI, Computational Electromagnetics, and Communication. (Email: engr.rehan@ustb.edu.pk)

Amin Sharafian received his M.Sc. degree in Control Engineering from the University of Qom in 2016 and his Ph.D. from the School of Automation at Shanghai Jiao Tong University (SJTU) in 2023. He has worked as a research associate at the University of Malaya and Shenzhen University. He has published several papers in well reputed journals and conferences. His research interests include fractional calculus, multi-agent systems, and cybersecurity. (Email: aminsharafian@szu.edu.cn)